J. Opt. Commun. 11 (1990) 3, 107–121

Journal of Optical Communications

Technology of Lapped Optical-Fiber Couplers

Valerio Annovazzi-Lodi, Silvano Donati

Summary

The technological steps for the fabrication of lapped fiber couplers are described in detail. Choice of materials and of working parameters as well as the diagnostic measurements of the process are discussed. The guidelines of design are outlined and data on the performances of manifactured wavelength-division-multiplexing couplers are reported.

1 Introduction

Optical fiber couplers have been developed about ten years ago [1] and, since then, they have become well-estabilised passive components of widespread use in communication networks and in sensors for the splitting and recombining of optical signals. In recent years, a large variety of special fiber couplers has been demonstrated, in which the splitting-ratio is either independent or selectively dependent on signal parameters such as wavelength, polarization, modal distribution, and (nonlinear) intensity.

As it is well known, there are three basic techniques currently used to fabricate fiber couplers, i.e.: *fused biconical*, *lapped* (or polished) and *micro-optic*. Several reviews [2–4] describe the fundamentals and compare the potentialities of each technique. However, let us briefly quote the commonly accepted advantages of the lapped-fiber technology as follows:

(i) the alteration of the fiber structure is minimal, which allows to work easily on special fibers, such as high-birefringence fibers, for polarization splitting and polarization mantaining couplers, and also on dissimilar fibers;

(ii) the open access to the interaction region allows the insertion of special intermediate layers (e.g., λ-selective, birefringent or nonlinear) thus increasing the design flexibility;

(iii) the inherent all-fiber structure has a negligible insertion loss.

On the other side, it shall be noted that environmentally related performances, ruggedness, volume production costs and yields of the lapped fiber technology are somewhere intermediate to those of the micro-optic and fused biconical technologies. Moreover, the fabrication of multiport (in excess of 2×2) couplers is difficult.

In this paper, we will focus on the fabrication of lapped fiber couplers, describing the choices of the abradants and working plate, the optimization of the process parameters, the measurements for process characterization, and the assembly procedure. For the design of the coupler geometry (minimum separation and curvature radius), we will follow the well-known results of Snyder's [5] weak-coupling theory. As an example, we finally report some typical data on wavelength-division-multiplexing couplers fabricated by the described process.

2 Coupler geometry and fiber preparation

In a lapped coupler, the fibers are arranged as shown in Fig. 1. The fibers are mounted on a holder with a curvature radius R and the clad is removed by lapping down to a minimum separation d_0 between the core axes.

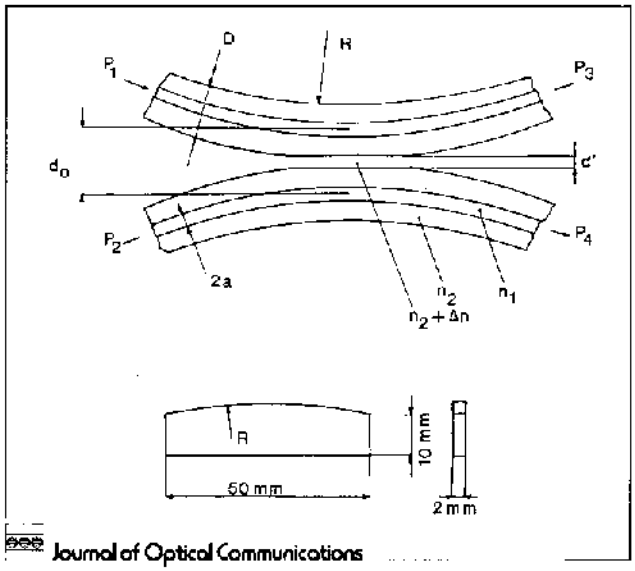

Fig. 1: Geometry of the coupler and of the fiber holder

Address of authors:

Dipartimento di Elettronica
Università di Pavia
27100 Pavia
Italy

Received 8 December 1989

The most commonly reported geometry of the holder is that of the groove-in-a-block [5–7], particularly suited for fabricating couplers with an adjustable splitting-ratio. For fixed couplers, intended for assembly in a package, we preferred to emboss the fiber onto the edge of a curved plate (Fig. 1), so that the working time is considerably shortened since there is much less material to remove.

Another fast procedure for working the fiber without a holder is to lay it under tension on a polishing-wheel [8]; however, special care is necessary to avoid breakage of the thinned fibers during the assemblying in the finished coupler.

The fiber is prepared for the lapping operation by stripping the coating (if any) with the help of a solvent (e.g. acetone) for a length equal to that of the holder, by aligning it on the centerline of the holder curved edge and cementing it with epoxy or other suitable resin, and finally by protecting it near the sharp holder edges with a drop of silicone resin.

The half-couplers are then ready for the lapping process described below. After this step, two half-couplers are mounted on a precision four-axis micropositioning stage and drawn together for the aligning procedure, using an index matching oil or glue between the fibers. The power outputs from ports 3 and 4 (Fig. 1) are monitored while launching first into port 1 and then into port 2. Small errors ($\approx 1\,\mu m$) in the machining depth are compensated for in this phase by acting on the fiber relative displacement. When the desired splitting ratio is obtained, fast UV-curable resin is applied to cement the coupler.

Finally, the coupler is encapsulated in the package by means of silicone resin, with special care to avoid undesired asymmetrical shrinking during polymerization and the associated variation of the splitting ratio.

3 Lapping procedure and abradant characterisation

To clamp in place the half-couplers and have a precisely lapped plane, in spite of their curved and blade-like shape, a fixture has been designed, consisting of two freely rotating coaxial cylindrical bodies, the inner one holding the half-coupler inside (Fig. 2). The external cylinder is secured to the moving arm of a standard rotating-plate lapping machine [9]. For all other details, the usual lapping practice [10] is employed.

Both alumina powders and diamond paste and slurry have been tested as abradants. Routine inspections of surface finish were carried out with a metallographic optical microscope, sometimes backed by electron microscopy and light scattering analysis. Process parameters were monitored as well as other factors such as the frequency of fiber breakage and the uniformity of removal speed.

Alumina powder is dispersed in water and used on a rigid synthetic cloth disc. Among different compositions commercially available, alumina of high purity α–γ phase has given the best results in terms of reproducibility, and surface finish. After several trials with different particle sizes, it has been determined that the 1 μm-size alumina is fully adequate for a single step lapping, yielding a short

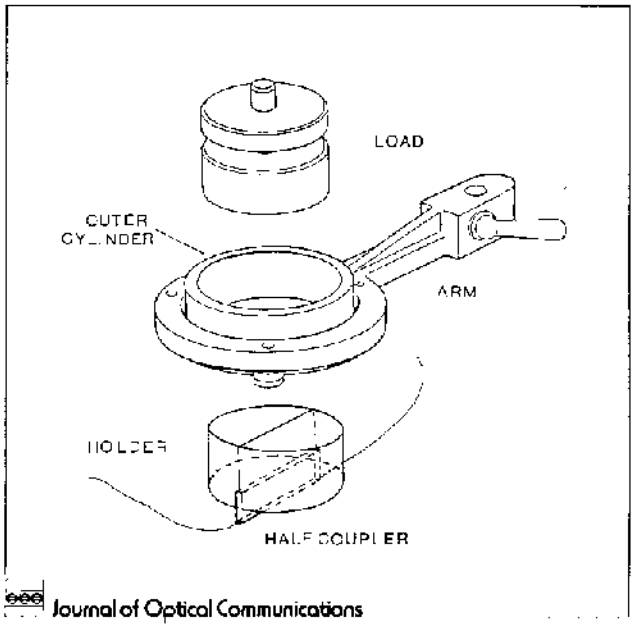

Fig. 2: Jig for lapping the half-couplers

(≈ 10 min.) machining time and yet a good finish quality even with no polishing.

It is interesting to correlate the removed depth s to the process variables, namely:

(i) disc speed v (turns/min);

(ii) pressure of the arm p (kg/cm^2);

(iii) alumina particle size ϕ (μm), and

(iv) working time t (hours).

Using flat samples of constant area (20 mm^2), we obtained the curves of s *versus* t reported in Fig. 3. The following empirical relation is found to fit well the experimental data:

$$s\ [\mu m] = h\ p^{\gamma} \phi^{\beta} v^{\alpha} t\ [\text{hours}] \qquad (1)$$

where the constants are given by

$$h = 1.2 \qquad \alpha = 1.0 \qquad \beta = 0.45 \qquad \gamma = 1.0. \qquad (2)$$

These values are the result of a best fit around: $v = 100$ turns/min, $p = 1$ kg/cm^2, $\phi = 1$ μm, and apply in the range $v = 30$–250 turns/min, $p = 0.5$–5 kg/cm^2, $\phi = 0.3$–5 μm.

For comparison, we also report the values of the same parameters for a diamond paste (1 μm-size) on lead-charged resin disc, around the same values of v, p, ϕ, i.e.:

$$h = 3.8 \qquad \alpha = 1.0 \qquad \beta = 1.25 \qquad \gamma = 0.5. \qquad (3)$$

The differences between (2) and (3) can be attributed not only to the different hardness of the abradants, but also to the different machining mechanism. Diamond particles are likely to be embedded into the disc, thus, exerting a true lapping action, while alumina moves loosely on the cloth and its action is closer to polishing.

With the 1μm-size diamond paste, a larger number of fiber breakages and some evidence of under-surface

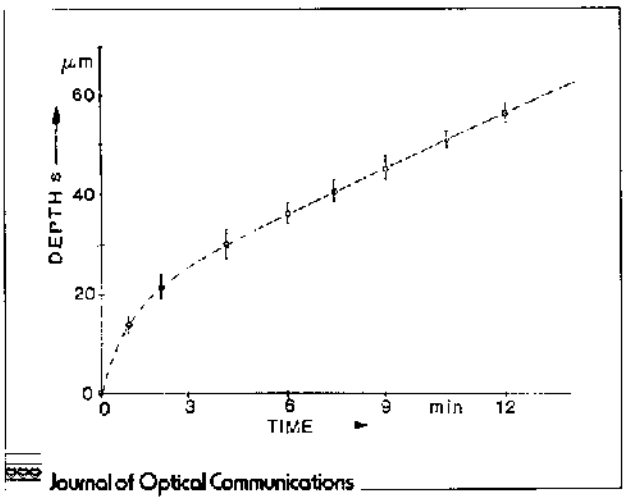

Fig. 3: Removed depth vs time for flat glass samples (20 mm² area) lapped with alumina (1 μm particle size) at different values of arm pressure p and plate speed v

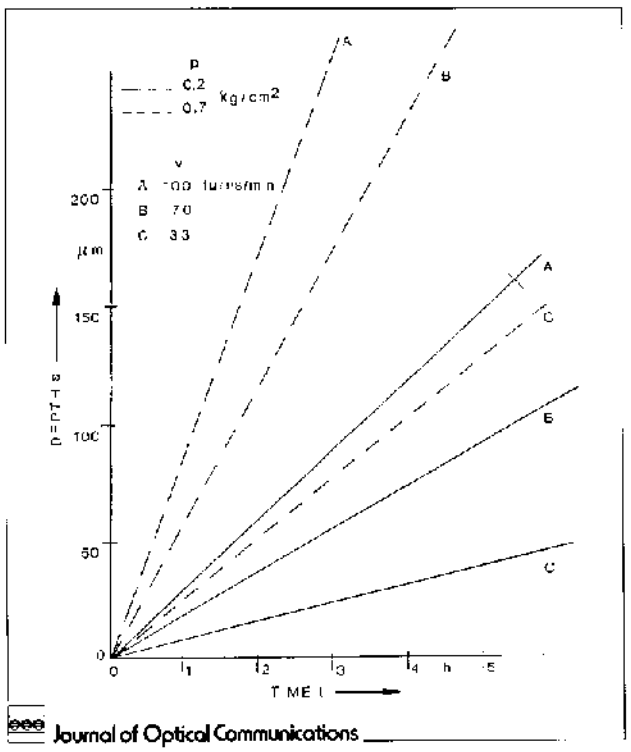

Fig. 4: Removed depth vs time for a silica fiber lapped at constant weight (W 300 g) and speed (v = 33 turns/min) with 1 μm alumina powder

damage [1] are found, while finer sizes yield too long machining times.

For the lapping of fibers mounted on half-couplers with 1μm-size alumina, we plot in Fig. 4 the removed depth s *versus* the working time t. The diagram is not linear at short times because the contact area between plate and fiber increases rapidly as lapping progresses, while the load on the tool and the disc speed are constant. At longer times, the regime becomes quasi-linear, and (1) holds with the following values of parameters and process variables:

$h = 1.2$, $\alpha = 0.3$, $\beta = 0.45$, $\gamma = 1.0$,
$v = 30$–250 turns/min, $p = 10$–50 kg/cm²,
ϕ 0.3–5 μm.

From the spread of the experimental data (Fig. 3), the working time allows to estimate the removed depth with an accuracy of 2–5 μm.

4 Process control and diagnostic measurements

An accurate control of the distance from the core/clad boundary is necessary in working the half-couplers, because the coupling factor varies appreciably as the minimum distance d_0 is changed on a 1 μm-scale for low-order coupling [2–5], and even more rapidly for high-order coupling. In addition, one shall take into account the tolerance on the fiber outer diameter, which is often well in excess of 1 μm in ordinary telecommunication fibers, and is usually found uncorrelated from sample to sample a few meters apart along the fiber.

A short cut to avoid this problem is obviously to overwork the fiber down to approximately the core/clad boundary, and insert between the two half-couplers a thick layer of index-matching resin (d′ in Fig. 1), squeezed to the appropriate thickness during the trimming operation. However, since the index of refraction varies during the resin polymerization and with aging, the trimming operation becomes more complicate and the long-time stability is objectionable; also, an unavoidable mismatch is expected *versus* wavelength. Therefore, only a relatively thin (of the order of 1 μm) index-matching layer is advisable.

Two kinds of diagnostics are required: *process* diagnostics, to be assessed once and necessary to establish the dependence of the removed depth on the process parameters, and *routine* diagnostics, necessary during the working of the half-couplers for lapping the fiber down to the design depth.

A destructive method has been used for the process diagnostics: the fiber is detached from its holder by a solvent and its thickness is measured under a metallographic microscope using a precision graticule scale, obtaining readings with a typical accuracy of ≈0.5 μm.

Other nondestructive diagnostics based on the measurement of the removed depth are unfortunately much less accurate and, in addition, they are affected by the outer diameter error. As said above, the calculation of the removed depth from the elapsed time yields an unacceptable error (in the range 2–5 μm), and this approach can then be used only as a first-step estimate, to rapidly remove most of the clad down to a safe distance from the fiber core. Another method, i.e., the correlation between the removed depth and the dimensions (axis-length) of the flat, ellipse-like section created on the fiber by lapping, is even less accurate (typ. 10 μm) because of the difficult visual identification of the ill-defined ellipse borderline.

More effective are those routines aimed to measure directly the actual distance of the lapped surface from the core. Among them, the technique of launching power in the half-coupler and measuring the transmitted power attenuation during lapping, originally proposed for diamond polishing [10], has been found difficult to implement with loose alumina on a cloth disc, because the fiber contact to the disc varies as the machine arm moves back and forth, and thus the output power exhibits strong fluctuations. To get reliable results, this method requires a

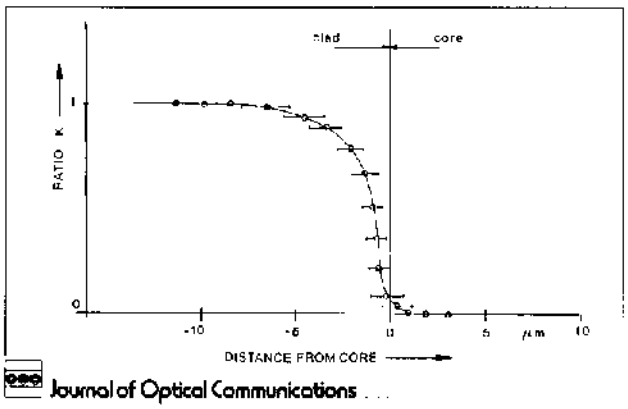

Fig. 5: Attenuation K vs distance due to an absobing tape applied onto the lapped fiber; the error bars include the concentricity error of the core

stable and suitable refractive index of the medium surrounding the fiber being lapped, which interferes with the preparation of the abradant suspension.

Instead, a precise but time-consuming method is that of measuring the power extracted from the lapped fiber by oils of different refractive indexes [13]. This method has been estimated accurate down to 0.5–1 μm. We use a modified version as a procedure sufficiently fast for routine working. With a rough estimate based on the elapsed working-time, the core is approached to within 5 μm, lapping is stopped and the half coupler is washed and dried. Power is launched at one fiber end while the trasmitted power P is measured at the other end. Then, an absorbing tape (a common tape with anaerobic glue) is pressed onto the lapped area to absorbe a well-defined and reproducible fraction of the power available for coupling, and the new power value P′ is measured. The ratio $K = P'/P$ is very sensitive to the distance from the core in the region around the core-clad interface, as shown in Fig. 5, and it gives a typical accuracy better than 1 μm on a useful working range in excess of 5 μm from the core boundary. The result of Fig. 5 is obtained by using a 633 nm He-Ne laser source and a 1300 nm monomode fiber (see Sect. 6). Because of the dependence on the normalized frequency v of the fiber, the working range can be extended using longer wavelengths (e.g. to about 8 μm with a 850 nm diode laser), with a corresponding decrease in accuracy.

5 Design rules

In the lapped-coupler geometry (Fig. 1), the design parameters to be selected are the minimum separation d_0 and the radius of curvature R. Restricting ourselves to couplers made with identical monomode fibers, and neglecting for the moment the effect of the intermediate layer ($d' = 0$), we apply the basic results of Snyder's low perturbation theory, which represents a good approximation in the weakly guiding regime [5, 14]. Our aim is to evaluate the typical values of the design parameters for different kinds of couplers, namely: fixed-ratio, WDM, mode- and polarization-splitters.

For an ideal lossless coupler, if P_1 is the power launched into port 1, the powers P_3 and P_4 at the direct and crossed ports (Fig. 1) are given by [4]:

$$P_4/P_1 = \eta = \sin^2(\pi L/2L_c), \quad (4)$$

$$P_3/P_1 = 1-\eta = \cos^2(\pi L/2L_c). \quad (5)$$

In these equations, L_c is the coupling length between the symmetrical and antisymmetrical modes of the two-core structure, and L is the effective interaction length; these quantities can be expressed in terms of d_0, R, and of the fiber geometrical parameters and guiding constants v, u, w as [5]:

$$L_c = \pi/2C_0 = \pi/[2(\pi\,\delta/w\,d\,a)^{1/2}\,(u^2/v^3)\exp(-w\,d_0/a)/K_1^2(w)] \quad (6)$$

$$L = (\pi R a/w)^{1/2} \quad (7)$$

where C_0 is the coupling coefficient evaluated at the minimum core distance d_0, and $\delta = 1 - n_2/n_1$.

Power-division couplers exploit the dependence of L_c on R and d_0. The coupler is usually tuned on the first order of coupling for the best stability. A weak dependence of the splitting ratio on λ is often desirable and can be obtained either by using dissimilar fibers or by properly selecting the curvature radius R, while the splitting ratio is trimmed by acting on d_0 [15].

Typical values of the effective interaction length L are of the order of 1 mm, while the length of the lapped region L (the major axis of the ellipse worked on the fiber) is about 10 mm, a value well in the reach of the lapping technology.

Couplers for the multiplexing of wavelength, polarization state or mode-order exploit the dependence of L_c on the guiding constants u, v and w. On the diagram of η vs. L, solutions are found when two curves have a maximum and a minimum of transmission in correspondence. This requires an effective interaction length L* given by:

$$L^* \cong L_{c1}L_{c2}/(L_{c1}-L_{c2}). \quad (8)$$

If the coupling lengths L_{c1} and L_{c2} are very close, the interaction length can be much larger than L_{c1} and L_{c2}, i.e., the first order of multiplexing corresponds to a high order of power-splitting coupling. Using in (9) the approximate expression $w \cong gv - 1$, where $g \simeq 1.14$ [16], L* is found as:

$$L^* \simeq (L_{c1}+L_{c2})/\{gAv[(1/(gv-1)-6/gv+(gv-4)/(1+0.25\,g^2v^2-2gv)]\}. \quad (9)$$

Typical values of L* are in the range of a few mm for a wavelength multiplexing of the second and third windows using a standard monomode fiber; also, the same order of magnitude is found for polarization multiplexers made with high-birefringence fibers.

Expressions for mode multiplexing are considerably more complicated, even in the simple case of LP_{01} and LP_{11} splitting. Interaction lengths of a few mm have been reported [17] for mode multiplexers based on dissimilar fibers; we have found this result consistent with a numerical evaluations and several experimental trials.

Nonlinear couplers exploit the dependence of the refractive index of a thin layer of nonlinear material, inserted between two standard half-couplers, on the intensity of the propagating wave. For a coupler structure with intermediate layer, it is found [12] that (4–7) still hold, provided that the coupling coefficient C_0 is multiplied by

a correction factor $1+h$. If d' and $n_{nl} = n_2 + \Delta n$ are the thickness and the refractive index of the nonlinear layer, respectively (see Fig. 1), in the assumption of weak perturbation one can find [12]:

$$h = vd'(n_{nl} - n_2)\,\pi/(w\lambda\sqrt{2\delta}). \qquad (10)$$

The nonlinear refractive index can be expressed in terms of the irradiance Ψ (W/cm^2) as: $n_{nl} = n_0 + \gamma\Psi$, where the third-order susceptivity γ is very low in silica (e.g., $\approx 10^{-10}$ cm^2/W) [18], but can reach $10^{-3} \div 10^{-4}$ cm^2/W in doped glasses and GaAs. A coupler designed for maximum transmission between ports 1 and 4 at low power will then switch to port 3 when power is increased beyond a specific level. For the coupler described in Section 6, with $L = 3$ mm and $d_0 = 9.1$ μm, switching is obtained for a variation of $d'\,\Delta n$ of the order of 0.01 μm. Using a suitable nonlinear glass, such a variation can be obtained with an input power ranging from a few hundred to a few thousand watts.

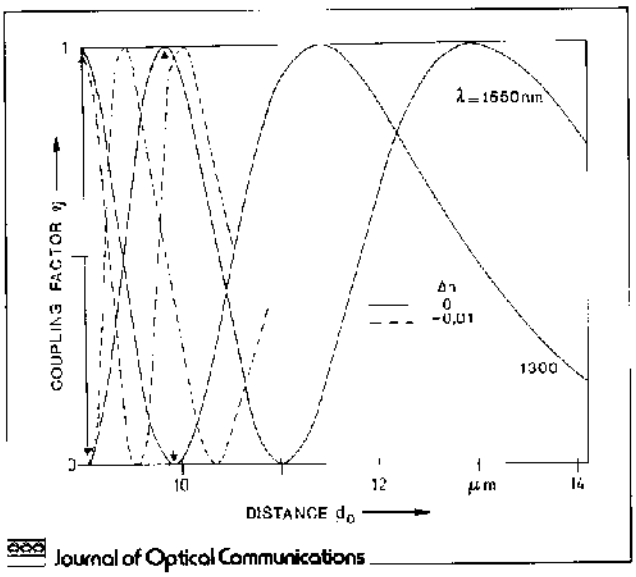

Fig. 6: Calculated coupling factor η *versus* core distance d_0, for R = 1 m (full lines); multiplexing between 1300 and 1550 nm is indicated by the arrows; dotted lines show the correction for a $\Delta n = -0.01$ matching layer ($d' = 0$ at $d_0 = 9.1$ μm)

6 WDM couplers

As an illustrative example of fabricated lapped-fiber couplers, we report some results on wavelength-division-multiplexing (WDM) couplers intended for the splitting at 1300 and 1550 nm. A standard monomode telecommunication fiber (Pirelli SM01) has been used, whose relevant parameters are: $\lambda_{cutoff} = 1230$ nm, core radius $a = 4.55$ μm, clad diameter $D = 125$ μm; $n_2 = 1.4514$, $n_1 = 1.4458$, (at 1300 nm). From numerical calculations of (4–7), the coupling factor η is evaluated as a function of the wavelength for several values of the parameters d_0 and R. Below a certain value of the curvature radius ($R < 0.8$ m), complete wavelength separation is not achieved, while several solutions for d_0 and R are found for $R > 0.9$ m. However, at higher orders of coupling, the control of lapping and trimming becomes critical as η varies rapidly with d_0. A typical plot of η *versus* d_0 is reported in Fig. 6 for R = 1 m (full lines), showing two possible choices of d_0 for the multiplexing between $\lambda = 1300$ and 1550 nm. Also plotted in Fig. 6. (dotted lines) is the effective η when the correction due to the matching layer between the fibres is taken into account ($\Delta n = -0.01$). Both 1300 and 1550 nm curves ar shifted, but their trend is essentially unchanged and it can be compensated for in the final trimming of the coupler. The calculated wavelength dependence of the coupling factor η is plotted in Fig. 7, for R = 1 m and $d_0 = 9.9$ μm (right-hand side arrows of Fig. 6).

Experimental points relative to a typical WDM coupler, representative of the performances obtained in a batch fabricated by lapping, are also reported in Fig. 7. The coupler was trimmend to match the working wavelengths, compensating for the effect of the intermediate layer and for machining errors. The spectral transmission response of the same device is reported in Fig. 8. The excess loss of the WDM coupler is 1 dB and the extinction ratio is 23 dB. Other average performances of the batch were: back isolation $P_2/P_1 < 35$ dB, error on nominal multiplexing wavelengths λ_1, λ_2: < 10 nm, error in wavelength separation $\Delta\lambda = \lambda_2 - \lambda_1 < 20$ nm.

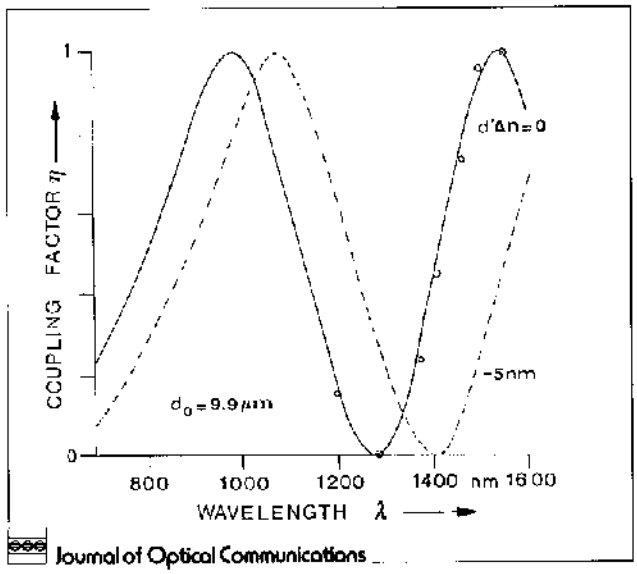

Fig. 7: Calculated coupling factor η *versus* wavelength λ (with R = 1 m, $d_0 = 9.9$ μm) for the WDM coupler with no intermediate layer (full lines) and with a thin intermediate layer $d'\Delta n = -5$ nm (dotted lines); experimental points are relative to the WDM coupler characterized in Fig. 8

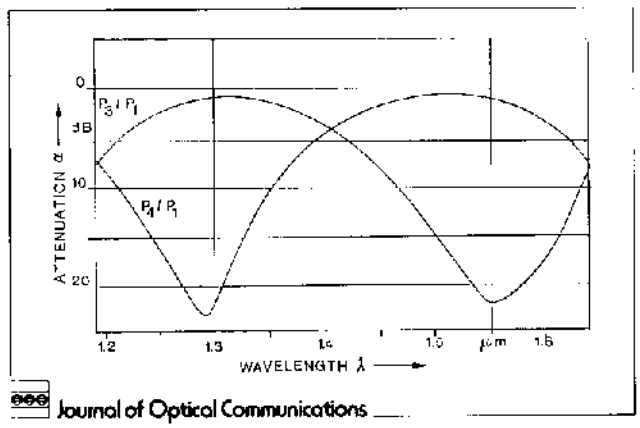

Fig. 8: Experimental result representative of a lapped WDM coupler: direct (P_3/P_1) and crossed (P_4/P_1) coupling factors *versus* wavelength

7 Acknowledgement

This work was supported by the Italian National Research Council under a MADESS contract.

References

[1] R. A. Bergh, G. Kotler, H. J. Shaw: 'Single-mode fiber optic directional coupler'; Electron. Lett. 16 (1980), 260–261
[2] A. K. Agarwal: 'Review of Optical Fiber Couplers': Fiber and Integrated Optics (1987) 1, 27–53
[3] J. M. Senior, S. D. Cusworth: 'Devices for wavelength multiplexing and demultiplexing'; IEE Proc. J. 136–3 (1989), 183–202
[4] J. Straus, B. Kawasaki: 'Passive Optical Components' in: 'Optical Fiber Transmission'; edited by E. E. Basch, H. Sams-Macmillan, Indianapolis 1987
[5] A. W. Snyder, J. D. Love: 'Optical Waveguide Theory'; Chapman and Hall, New York, Chapter 18, 1983
[6] M. J. F. Digonnet, H. J. Shaw: 'Analysis of a tunable single-mode optical fiber coupler'; IEEE JQE'18–4 (1982), 746–754
[7] S. T. Nicholls: 'Automatic manifacture of polished single-mode-fiber directional couplers', Elec. Lett. 21–9 (1985), 825–826
[8] C. D. Hussey, J. D. Minelly: 'Optical fiber polishing with a motor driven polishing wheel'; Electron. Lett. 24 (1988), 805–807
[9] Kent-3 Automatic lapping and polishing unit, Engis Ltd., U.K.
[10] G. W. Finn, W. J. A. Powell: 'Cutting and polishing of optical and electronic materials'; 2nd ed., IOP Publishing, Accord, 1983
[11] P. P. Hed, D. F. Edwards, J. B. Davis: 'Surface damage in optical materials: origin, measurement and removal'; Lawrence Livermore Nat. Lab. UCRL 99548–1, March 1989
[12] V. Annovazzi-Lodi: 'Analysis of lapped fiber couplers with an intermediate layer'; IEEE Photon. Tech. Lett. 1 (1989), 381–383.
[13] M. J. Digonnet et al.: 'Measurement of the core proximity in polished fiber substrates and couplers'; Opt. Lett. 10–9 (1985), 463–465
[14] A. Ankiewitz, A. W. Snyder, X. Zheng: 'Coupling between parallel optical fiber cores: critical examination'; IEEE JLT LT–4 (1986), 1317–1323
[15] M. Digonnet, H. J. Shaw: 'Wavelength multiplexing in single-mode fiber couplers'; Appl. Opt. 22–3 (1983), 484–491
[16] H. D. Rudolph, E. G. Neumann: 'Approximations for the eigenvalues of the fundamental mode of a step index glass fiber waveguide'; Nachr.-Techn. Z. 29 (1976), 328–329
[17] W. Y. Sorin, B. Y. Kim, H. J. Shaw: 'Highly selective evanescent modal filter for two-mode optical fibers'; Opt. Lett. 11–9 (1986), 581–583
[18] G. I. Stegeman, R. H. Stolen: 'Waveguides and fibers for nonlinear optics', J.O.S.A. B 6–4 (1989), 652–662